



Cite this: *Chem. Commun.*, 2024, **60**, 1012

Received 27th September 2023,
Accepted 12th December 2023

DOI: 10.1039/d3cc04802k

rsc.li/chemcomm

Illumination into an electron paramagnetic resonance (EPR) spectrometer is commonly carried out through the optical window, perpendicular to the sample and magnetic field. Here we show that significant improvements can be obtained by using the walls of the EPR tube as a light guide, with the light scattered only around the sample-containing area.

Many chemical reactions and processes have mechanisms involving species with unpaired electrons, either as reactants, products, intermediates or catalysts. These are measurable by electron paramagnetic resonance (EPR), and examples include organic radicals,^{1,2} nitroxides,³ metal centres/clusters,⁴ and excited triplet states. The processes involving the generation or removal of these species may be initiated by light. Common examples include the study of polymerisation,¹ photosensitisation for the generation of singlet oxygen,³ catalytic,² or biocatalytic processes. To measure the changes in EPR active species caused by illumination, the sample can be irradiated *ex situ*, then inserted into the spectrometer and a spectrum recorded. Alternatively, the sample can be irradiated *in situ* within the EPR spectrometer, before or during the acquisition of spectra.

Ex situ illumination is easy to achieve, and many different light sources, including light emitting diodes (LEDs)^{1,2} and lasers,³ have been reported. However, this method prohibits acquisition of the EPR spectrum during irradiation and can only measure changes that persist on a timescale longer than

the time taken to place the sample in the spectrometer and record the measurement. Consequently, EPR active species with short lifetimes may be missed. For this reason, it is often advantageous or necessary to measure the sample under *in situ* illumination, where EPR active species can be detected as soon as they are generated. Examples of this type of illumination typically include illumination through an optical window,^{4–6} or *via* optical fibre.^{7,8} Here, the limiting time scale is the time taken for the measurement to be recorded, which can be on the order of ns to ms for time resolved transient EPR (trEPR) methods, which use a pulsed laser as the light source.⁹ Alternatively for species with longer lifetimes, on the order of seconds to hours, a time course of continuous wave (CW) EPR experiments can be used to record the formation and decay of the species. Paramagnetic species under continuous illumination can be recorded at steady state, such experiments have been reported with xenon lamps,^{10–14} solar simulators,¹⁰ lasers,^{15–18} or LEDs.^{13,19–22}

Providing sufficient optical access to the sample within the EPR resonator for *in situ* illumination can be challenging. Direct illumination through the optical window of a resonator gives a straight-forward light path. However, the design of many EPR resonators means that the window is either protected by a microwave-filtering mesh that reduces the amount of light entering the sample, or is very small (mm in diameter) or both. Moreover, irradiation from the side can preclude uniform illumination across the sample itself, with the side of the tube closest to the illumination window receiving greater illumination. A small optical window may also prevent complete illumination along the length of the sample. In EPR spectroscopy, samples are often measured in solid phases, such as frozen solutions, where there is no fluid motion to mix the sample, amplifying the negative effects of only illuminating a portion of the sample. Light delivered *via* the optical window is incident on the side of the sample tube – this is usually curved leading to refraction of the light, further reducing the amount of light reaching the sample. In cases where a cryostat is used, light must pass through a series of flat quartz (Spectrosil B) windows (*e.g.* Oxford Instruments CF935 or the CF-VTC Cryogenic

^a Department of Chemistry, School of Natural Sciences, The University of Manchester, Oxford Road, Manchester, M13 9PL, UK.

E-mail: alice.bowen@manchester.ac.uk, a.golovanov@manchester.ac.uk

^b Photon Science Institute, School of Natural Sciences, The University of Manchester, Oxford Road, Manchester, M13 9PL, UK

^c National Research Facility for Electron Paramagnetic Resonance Spectroscopy, School of Natural Sciences, The University of Manchester, Oxford Road, Manchester, M13 9PL, UK

† Electronic supplementary information (ESI) available: see DOI: <https://doi.org/10.1039/d3cc04802k>. The raw data and data processing for the EPR data are available from the University of Manchester repository: see DOI: <https://doi.org/10.48420/23749047>.

‡ These authors contributed equally to this work.



cryostat for EPR) or pass through a curved quartz insert (e.g. Oxford Instruments ESR900). In both cases reflection and refraction at these layers of quartz leads to further loss of light intensity. To overcome this light intensity loss, high-powered light sources e.g. mercury arc lamps or lasers can be used. These can cause localised heating or damage which may be detrimental to sample, resonator, and optical windows.

Fibre optics inserted directly into a sample tube can also be used to illuminate EPR sample from above. However, their use incurs heavy optical losses at the point of coupling, necessitating high power sources that can in turn impact the integrity of the fibre. If the sample is optically dense, then again, the part closest to the end of the fibre receives more light and illumination is attenuated through the sample, leading to reaction non-uniformity along the length.

Recent work by the authors has suggested a new method of *in situ* illumination of samples in related technique, nuclear magnetic resonance (NMR) spectroscopy. The proposed approach (called the NMRtorch)^{23,24} works by positioning an LED light source directly on top of the specially modified sample tube, with the thick walls of the tube itself acting as a light guide. The light around the area containing the sample is however scattered, illuminating the sample from the outside.^{23,24} This arrangement benefits from the matching cross-section area of the tube end and light emitting surface, minimising the transfer losses and avoiding intermediary optical components such as optical fibres, thus maximising the intensity of light delivered to the sample.^{23,24} In early versions of the NMRtorch^{23,24} the light scattering centres were introduced *via* abrasive etching on the outside surface of the glass.

In this study we explored how the NMRtorch design principles can be transferred and adapted for efficient sample illumination in EPR. First, using the same LED light source, we explored *ex situ* the amount of light delivered to the top of EPR sample tube when using the direct NMRtorch-like illumination, and when the same source was connected *via* a standard optical fibre. Light intensity in both configurations was measured by a light meter (UPRtek, PG200N). Light losses using the optical fibre were $\sim 80\%$ ($3698 \pm 245 \text{ mW m}^{-2}$ at the end of the fibre compared to $18711 \pm 897 \text{ mW m}^{-2}$ at the outlet of the LED). This suggests the direct illumination approach without optical fibre delivers around 5 times more light to the end of the EPR tube. Another issue is how to distribute light delivered to the tube around the sample. In NMR probeheads usually there is no extra space for any additional light-scattering material on the exterior of the sample tubes, whereas in continuous wave EPR the resonators are typically able to allow for a thin layer of wrapping on the outside of the tube, presenting an opportunity to further modify the way how light scattering around the sample volume can be achieved. Here, we have explored the use of PTFE tape and compared this to abrasive etching. These novel EPR illumination approaches are benchmarked against perpendicular illumination through resonator window using the same light source closely-positioned to the optical window. To analyse the effectiveness of these illumination strategies, we used the photogenerated radical formation of the riboflavin derivative flavin mononucleotide

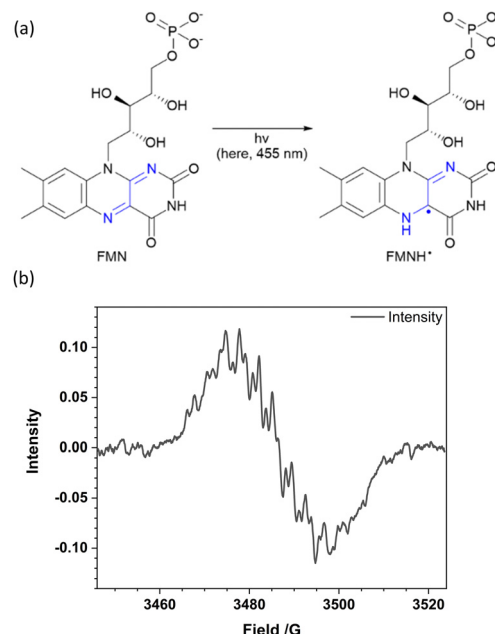


Fig. 1 (a) Structure of FMN and its semiquinone form FMNH[·] generated upon illumination. (b) EPR signal of FMNH[·] radical. Measurement parameters: microwave power 20 dB (2.2 mW), modulation amplitude 0.5 G, time constant 81.92ms, conversion time 5.01 ms, sweep time 20 s, receiver gain 30 dB and an average microwave frequency of 9.83GHz.

(FMN, Fig. 1(a)), suspended in an agarose-gel matrix. This has previously been demonstrated as a model system for radical generation, as the matrix stabilises the protonated radical form FMNH[·] generated upon illumination, allowing concentrations sufficient for detection *via* EPR to be formed.²⁵ The concentration of the radical formed, and the rate at which it is formed, are proportional to the amount of delivered light, allowing assessment of the different illumination approaches. The formation of the FMNH[·] radical was identified from the spectral EPR signal (Fig. 1(b)).

The agarose gel matrix containing flavin was prepared under darkness according to the protocol of Rostas *et al.*²⁵ Deionised H₂O was bubbled with argon for 10 minutes to remove oxygen before 2.5% (w/v) agarose (Fisher, BPE1356-100) and 25 mM FMN sodium salt hydrate (Sigma-Aldrich, F6750) was dissolved with continued argon flow and stirring. Argon flow was stopped, and the solution and 3 mm heavy-walled fused quartz EPR tubes (inner diameter 1 mm, Ilmasil[®] PN, QSIL, Germany) heated to 80 °C in a water bath. Aliquots of the solution were transferred to the tubes to a fill height of 4 cm. This fill height was chosen to be larger than the active region of the CW EPR resonator. The filled tubes were removed from the water bath and cooled to room temperature, resulting in gelation of the agarose FMN mixture.

CW X Band (9.8 GHz) EPR measurements were carried out at room temperature using a Bruker EMXMicro EPR spectrometer equipped with a Bruker ER4112SHQ-X resonator without a cryostat fitted. All samples were measured in non-saturating conditions as confirmed by power dependence measurements. Field offset correction was carried out by comparison against the Bruker Strong Pitch standard ($g = 2.0028$). Photoexcitation



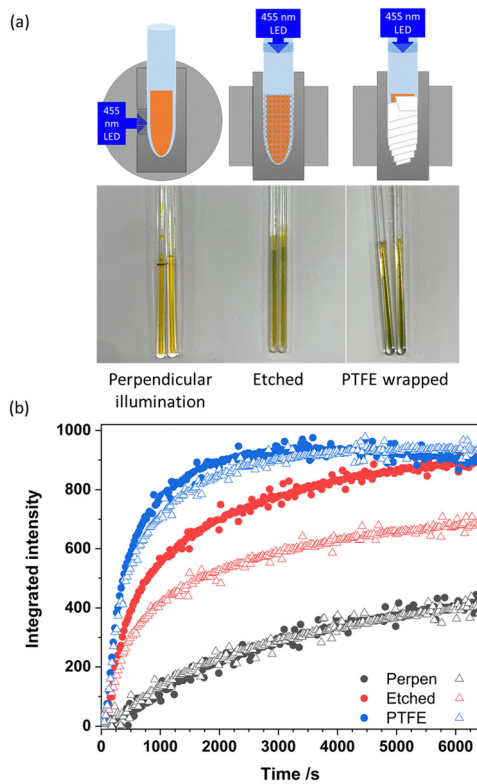


Fig. 2 (a) Schematic diagram of three illumination techniques used here for comparison: with etched tube, tube wrapped with PTFE tape, and direct perpendicular illumination of unmodified sample tube, photograph of irradiated samples. (b) Plot of integrated signal intensity against irradiation time. Closed circles correspond to the first sample run, open triangles to the second independent sample run. Measurement parameters used in the 2D EPR measurements were: microwave power 20 dB (2.2 mW), modulation amplitude 10 G, this overmodulated the signal to remove the strong hyperfine coupling seen in Fig. 1, time constant 81.92 ms, conversion time 5.01 ms, sweep time 20 s, receiver gain 30 dB and an average microwave frequency of 9.83GHz.

was achieved using the same 455 nm LED (Thorlabs M455F3, LEDD1B power supply) illumination source, in several arrangements. In each case the LED was switched on after the completion of 3 scans, and the signal was monitored for 256 sweeps (approx. 100 minutes).

Benchmarking experiments used a commonly-used arrangement – the LED placed 5 cm away from the optical window of the resonator providing perpendicular excitation (Fig. 2(a), right). The results showed a slow formation of the radical over the experiment (Fig. 2(b) black points). Recorded spectra were baseline corrected and the second integral was plotted against time. The initial rate radical formation was determined from a local regression fitted to the start of each dataset and reported in Table 1.

FMN in the neutral state is yellow however when it enters the protonated radical form FMNH^{\bullet} a colour change to green is observed. Under perpendicular illumination though the window this colour change was subtle and observed in the centre of the sample indicating that only a small region of the sample had been weakly illuminated (Fig. 2(a) left). The results obtained from this method were very reproducible as shown in Fig. 2(b).

Table 1 Determined rates of radical formation as increase in integrated signal intensity (SI) per unit time to demonstrate light intensity

	Initial rate of radical formation ($\text{}/\text{s}^{-1}$) (error based on one standard deviation)	
	Sample 1	Sample 2
Perpendicular illumination	0.01 (± 0.10)	0.19 (± 0.12)
Etched tube	1.04 (± 0.10)	0.69 (± 0.11)
PTFE wrapped	1.85 (± 0.12)	1.62 (± 0.10)

Following the protocol of the NMRtorch two other illumination conditions were trialled; in both cases the LED source was mounted directly on top of tube for longitudinal illumination. As the inner diameter of the light outlet of this LED source was only marginally larger than the 3 mm tube outer diameter, the open end of the tube could simply be inserted inside the outlet. To prevent direct contact of the top of the tube with the otherwise unprotected LED, we used a small collar formed from suitably sized silicon tubing (Fig. S1, ESI[†]) which restricted the depth to which the tube end was inserted inside the light source, additionally allowing the source to rest at the top of the tube inserted into the resonator, without need for any further support. To achieve the required light scattering around the sample area, preferentially illuminating the sample volume, two approaches were investigated (Fig. 2(a), centre and right). First, we used the same technique described in the NMRtorch work, abrasively etching lightly with sandpaper the exterior surface of the EPR tube covering the bottom 4 cm length where the sample was placed. While this method led to an overall larger signal at the end of the experiment compared to perpendicular illumination, the reproducibility between two different tubes was limited, likely due to poorly-controlled manually-performed etchings (Fig. 2(b) red points): the variation of initial rate of radical formation between two otherwise identical samples in Table 1 was significant. As many photoinitiated EPR studies are concerned with measuring absolute radical concentration as a function of sample conditions, quantitative EPR or spin-counting,²⁶ the consistency of the etching could be improved by automatic machining of the etched tubes; alternatively, or the same tube can be reused for different samples.

Given that EPR resonators are less restrictive regarding the outside sample tube diameter than NMR probeheads, we tried to achieve light scattering by wrapping two layers of white PTFE tape (BS7786:1995 Grade L EN-751; 12 mm width, 0.075 mm thick) around the sample area. The first layer was pressed hard into the glass to minimise amount of air trapped between the glass and the tape, turning the inner reflection at the outer glass interface into scattering, whereas the second layer was applied without excessive slack as a secondary light-reflective barrier. This methodology produced the deepest green colour in the samples Fig. 2(a), the largest overall signal intensity, and the fastest initial rate of radical formation (Fig. 2(b), blue points and Table 1). This method of illumination was also found to be significantly more reproducible between samples prepared in different tubes. It also does not require permanent modification of the EPR tubes which allows them to be reused for other

experiments. Interestingly, the deepest green colour was concentrated at the base of the sample, further away from the light source. This may be due to the curved base of the tube scattering more light. Having more light towards the end of EPR tube may be advantageous, as it is easy to position the bottom of the sample consistently in a resonator or a cryostat. Further experimentation with the interplay between sample volume, etching patterns and/or the length of PTFE wrapped area may help to improve the uniformity of illumination along the length of the sample, and other light-scattering coatings and patterns can also be envisaged that would give more uniform light distribution for cases where uniformity is critical.

The results presented here clearly show that using NMRtorch longitudinal illumination principles provides much stronger and more efficient sample illumination compared to typical perpendicular illumination *via* the optical window. The methodology can be easily applied using a commercially available LEDs and commercially available quartz tubing cut into suitable lengths and sealed at one end by a glass blower. Using the longitudinal illumination routed *via* the walls of the tube itself yielded a significant increase in both initial rate of radical generation and final radical concentration. The most efficient light scattering around the sample, with the highest rate of radical generation and high reproducibility, was achieved by just wrapping the sample tube around sample area in PTFE tape. Exploring other light-scattering strategies may further increase the efficiency of illumination and uniformity. This approach will likely have important future applications in the study of a wide range of photo-initiated reactions and catalytic processes.

A. M. B. is grateful to The Royal Society and EPSRC for a Dorothy Hodgkin Fellowship (DH160004 and DHF|R|221018), and the University of Manchester for a Dame Kathleen Ollerenshaw Fellowship. A. M. B. also thanks the Royal Society of Chemistry for a Community for Analytical and Measurement Science (CAMS) fellowship (2020 ACTF ref. 600310/09). A. M. B. and A. W. W. thank The Royal Society for the research grant and enhanced research expenses (RGF|EA|201050 and RF|ERE|210351). A. M. B. is also grateful for support received from the Interstellar Scheme of the New York Academy of Sciences and The Japan Agency for Medical Research and Development (AMED). The authors acknowledge the EPSRC New Horizons EP/V04835X/1 funding, and the EPSRC funded National Research facility for EPR at the University of Manchester (EP/W014521/1, NS/A000055/1, EP/V035231/1 and EP/S033181/1), for use of facility access and support. A CC BY or equivalent license is applied to the Author Accepted Manuscript arising from this submission.

Conflicts of interest

There are no conflicts to declare.

References

- 1 B. L. S. Vicentin, R. F. Peron, B. C. Amorim, D. D. A. Buelvas, E. Di Mauro, H. O. I. Borges and M. G. Hoeppner, *J. Appl. Spectrosc.*, 2019, **86**, 244–249.
- 2 X.-A. Liang, L. Niu, S. Wang, J. Liu and A. Lei, *Org. Lett.*, 2019, **21**, 2441–2444.
- 3 T. Takajo, Y. Kurihara, K. Iwase, D. Miyake, K. Tsuchida and K. Anzai, *Chem. Pharm. Bull.*, 2020, **68**, 150–154.
- 4 A. Lee, M. Vörös, W. M. Dose, J. Niklas, O. Poluektov, R. D. Schaller, H. Iddir, V. A. Maroni, E. Lee, B. Ingram, L. A. Curtiss and C. S. Johnson, *Nat. Commun.*, 2019, **10**, 4946.
- 5 C. Mendoza, A. Désert, L. Khrouz, C. A. Páez, S. Parola and B. Heinrichs, *Environ. Sci. Pollut. Res.*, 2021, **28**, 25124–25129.
- 6 Q. Jiang, E. Fangjie, J. Tian, J. Yang, J. Zhang and Y. Cheng, *ACS Appl. Mater. Interfaces*, 2020, **12**, 16150–16158.
- 7 A. Bertran, K. B. Henbest, M. De Zotti, M. Gobbo, C. R. Timmel, M. Di Valentin and A. M. Bowen, *J. Phys. Chem. Lett.*, 2021, **12**, 80–85.
- 8 S. V. Nistor and A. C. Joita, *Appl. Magn. Reson.*, 2020, **51**, 287–296.
- 9 S. Weber, in *eMagRes*, ed. R. L. Wasylishen, R. K. Harris, Wiley, 2017, **6**, pp. 255–270.
- 10 Z.-Y. Yan, J. Chen, J. Shao, Z.-Q. Jiao, T.-S. Tang, M. Tang, Z.-G. Sheng, L. Mao, R. Huang, C.-H. Huang, Z.-H. Zhang, H.-M. Su and B.-Z. Zhu, *Free Radical Biol. Med.*, 2021, **171**, 69–79.
- 11 R. Kaptein, K. Dijkstra and K. Nicolay, *Nature*, 1978, **274**, 293–294.
- 12 K. Yao, A. Bertran, J. Morgan, S. M. Hare, N. H. Rees, A. M. Kenwright, K. Edkins, A. M. Bowen and N. J. Farrer, *Dalton Trans.*, 2019, **48**, 6416–6420.
- 13 E. Cerrato, M. C. Paganini and E. Giamello, *J. Photochem. Photobiol. A*, 2020, **397**, 112531.
- 14 K. Yao, A. Bertran, A. Howarth, J. M. Goicoechea, S. M. Hare, N. H. Rees, M. Foroozandeh, A. M. Bowen and N. J. Farrer, *Chem. Commun.*, 2019, **55**, 11287–11290.
- 15 O. G. Poluektov, S. Filippone, N. Martín, A. Sperlich, C. Deibel and V. Dyakonov, *J. Phys. Chem. B*, 2010, **114**, 14426–14429.
- 16 N. Y. Garces, L. Wang, N. C. Giles, L. E. Halliburton, G. Cantwell and D. B. Eason, *J. Appl. Phys.*, 2003, **94**, 519–524.
- 17 M. Zhang, J. Yao, M. Arif, B. Qiu, H. Yin, X. Liu and S.-M. Chen, *Appl. Surface Sci.*, 2020, **526**, 145749.
- 18 M. Buryi, V. Laguta, M. Fasoli, F. Moretti, K. Jurek, M. Trubitsyn, M. Volnianskii, S. Nagorny, V. Shlegel, A. Vedda and M. Nikl, *J. Lumin.*, 2019, **205**, 457–466.
- 19 Z. Lu, X. Fu, H. Yang, Y. Zhao, L. Xiao and L. Hou, *Polym. Chem.*, 2021, **12**, 183–188.
- 20 D. Dvoranová, Z. Barbierová, M. Mazur, E. I. García-López, G. Marcí, K. Lušpáí and V. Brezová, *J. Photochem. Photobiol. A*, 2019, **375**, 100–113.
- 21 M. Krajewski, P. Piotrowski, W. Mech, K. P. Korona, J. Wojtkiewicz, M. Pilch, A. Kaim, A. Drabińska and M. Kamińska, *Materials*, 2022, **15**, 6908.
- 22 G. Marcí, E. I. García-López, F. R. Pomilla, L. Palmisano, A. Zaffora, M. Santamaría, I. Krivtsov, M. Ilkaeva, Z. Barbierová and V. Brezová, *Catal. Today*, 2019, **328**, 21–28.
- 23 J. E. Bramham and A. P. Golovanov, *Commun. Chem.*, 2022, **5**, 90.
- 24 J. E. Bramham, M. Zalar and A. P. Golovanov, *Chem. Commun.*, 2022, **58**, 11973–11976.
- 25 A. Rostas, C. Einholz, B. Illarionov, L. Heidinger, T. A. Said, A. Bauss, M. Fischer, A. Bacher, S. Weber and E. Schleicher, *J. Am. Chem. Soc.*, 2018, **140**, 16521–16527.
- 26 G. R. Eaton, S. S. Eaton, D. P. Barr and R. T. Weber, *Quantitative EPR: A Practitioners Guide*, Springer, Vienna, 2010, pp. 25–36.

